Supporting Information

1 Methods

1.1 Materials

(−)-3-(Trifluoroacetyl)camphor (98%) was purchased from Sigma-Aldrich Co. LLC. Europium(III) chloride hexahydrate (99.9%) was purchased from FUJIFILM Wako Pure Chemical Corporation. Tetraethylammonium chloride (>98.0%(T)), (+)-camphor (98.0%(GC)). sodium hydride (60% dispersion in Paraffin Liquid), ethylpentafluoropropionate (98.0%(GC)), and Coumarin 102 (> 97.0% (HPLC) (N)) were purchased from TCI chemicals.

1.2 General methods

^{1}H-NMR spectrum was recorded in chloroform-*d* using a JEOL ECS-400 spectrometer. Tetramethylsilane (TMS, δ_H = 0 ppm) was used as internal standards. Elemental analyses were performed using MICRO CORDER JM10. Electrospray ionization (ESI) mass spectrometry was conducted on a JEOL JMS-T100 LP instrument. MALDI-TOF mass spectra were recorded on a Bruker autoflex® maX spectrometer. Transmission and absorption spectra were measured using a JASCO V-670 spectrometer. Fourier transform infrared (FT-IR) spectra were measured using a JASCO FT/IR-4600 instrument. Emission spectra (λ_{ex} = 350 nm), excitation spectra (λ_{em} = 612 nm) and emission decay profiles (λ_{ex} = 356 nm, λ_{em} = 612 nm) were obtained using a Horiba FluoroLog®3 spectrofluorometer. Emission quantum yields (λ_{ex}=350 nm) were obtained using EDINBURGH FLS1000. CPL spectra were recorded on a JASCO CPL-300 circularly polarized luminescence spectrometer, which were averaged over 12 measurements. The wavelength of the CPL spectra was corrected for the emission peak measured with a HORIBA Fluorolog-3 spectrofluorometer. The photographs of CPL were taken following the method described in a previous report[19] using a digital camera equipped with a short-pass filter (< 600 nm, Edmund optics), a rotatable λ/4 plate (Thorlabs, WPQSM05-588), and a linear polarizer (LP, Thorlabs, LPVISE100-A). The discrimination between L-CPL and R-CPL was achieved using a combination of the plate and LP. These two detection states were determined by the specific rotation angles of the plate relative to the transmission axis of the LP. For L-

CPL detection, the fast axis of the plate was set at -45° relative to the LP axis to convert the L-CPL component into linearly polarized light that passes through the LP. Conversely, for R-CPL detection, the plate was rotated to +45° to convert the R-CPL component into the transmissive linear polarization state. By switching between these two angles (±45°), the emission intensity of each helicity was selectively observed. To record the images with different polarization ratios shown in Figure 4, the rotation angle of the λ/4 plate (θ) was incrementally adjusted between –45° and +45° relative to the transmission axis of the LP. Specifically, the images were captured at θ = –45°, –15°, 0°, +15°, and +45°. At θ = 0°, the plate acts as a simple birefringent medium with its axes aligned with the LP, allowing an equal ratio of L- and R-CPL components to be processed. These intermediate angles provide a visual representation of the transition between L- and R-CPL dominant states

Time-resolved emission spectra were obtained by an optical setup mainly consisting of laser diode(PLP-10, Hamamatsu Photonics Co., Ltd.), a 3D Raman confocal microscope system, a high-resolution monochromator, and a streak camera. The particle was directly dispersed on a copper substrate. It was excited with an OPO (Chameleon Vision-S, Coherent, Inc.) pumped by a pulsed Ti: Sapphire laser with an emission wavelength at 365 nm. The 3D Raman confocal microscope system (Nanofinder 30, Tokyo instruments, Inc.) functions as a real-time imaging spectrometer to monitor the emission from single-particle phosphor under the 375nm laser excitation. The reflected optical signals, collected through a fluorescence microscope (BX51M, Olympus Co., Ltd.) were directed to a high-resolution monochromator (SpectraPro HRS-300, Princeton Instruments, Inc.) and a streak camera (C14831-110, Hamamatsu Photonics Co., Ltd.). The emission spectral range was monitored between 452 nm and 583 nm with a 100 g mm^{-1} grating.

1.3 Preparation of (+)-3-(pentafluoropropionyl)camphorate (+pfc)

(+)-3-(pentafluoropropionyl)camphorate was prepared using the same procedure described in previous report (Figure S1).[21]

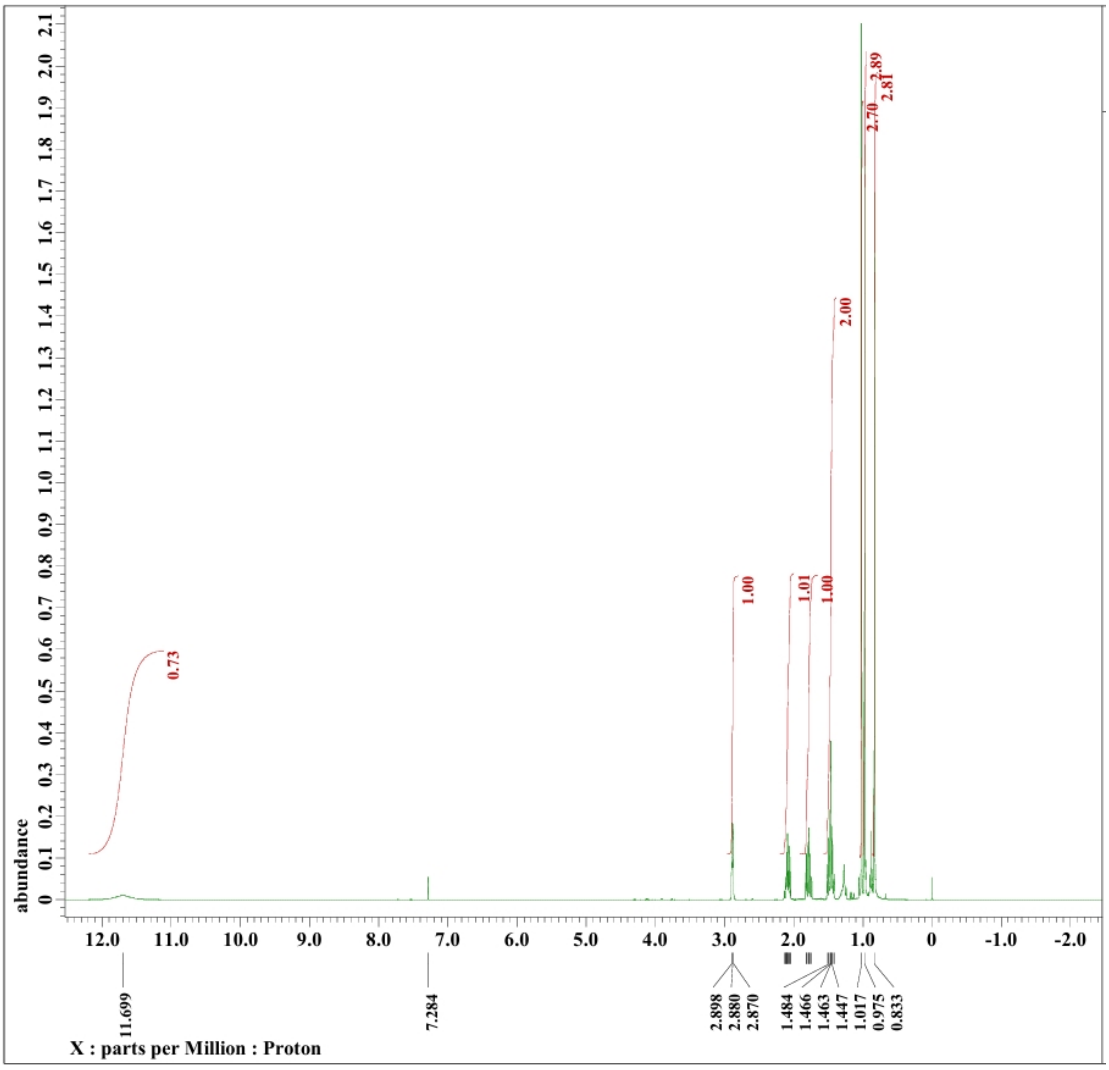

Figure S1. ^{1}H NMR spectrum of +pfc ligand in chloroform-*d*.

1.4 Preparation of TEA[Eu(−tfc)$_4$] (TEA: tetraethylammonium)

(−)-3-(trifluoroacetyl)camphor (534 mg, 2.2 mmol) was dissolved in ethanol (5 mL). Ethanol solutions (5 mL) of tetraethylammonium chloride (244 mg, 1.5 mmol) and europium(III) chloride hexahydrate (276 mg, 0.75 mmol) were added dropwise to the solution. The saturated ethanol solution of sodium hydroxide was added dropwise to the mixture to adjust the pH to 7. After stirring 1 h, white precipitate was removed from the reaction

mixture. The reaction solution was evaporated to yield a light-yellow powder. The obtained powder was recrystallized from acetonitrile to afford light-yellow crystals.

Yield: 186.3 mg, 19.4%.

Elemental analysis: calcd. for $C_{56}H_{76}EuF_{12}NO_8$, C 52.92, H 6.03, N 1.10; found, C 52.66, H 5.95, N 1.15%

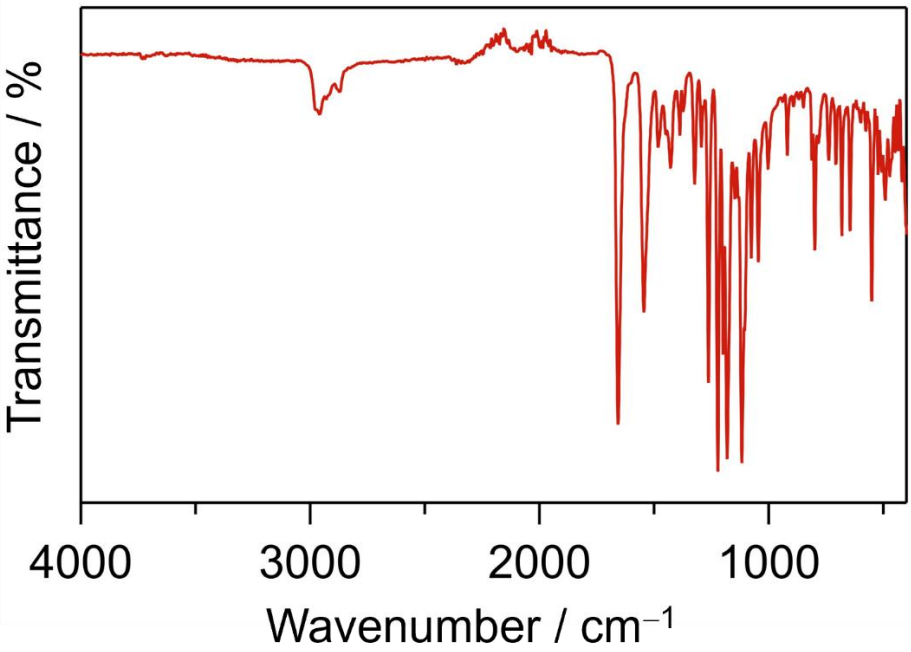

Figure S2. IR spectrum of TEA[Eu(−tfc)$_4$].

1.5 Preparation of TEA[Eu(+pfc)$_4$] (TEA: tetraethylammonium)

(+)-3-(pentafluoropropionyl)camphor (639 mg, 2.1 mmol) was dissolved in ethanol (5 mL). Ethanol solutions (5 mL) of tetraethylammonium chloride (246 mg, 1.5 mmol) and europium(III) chloride hexahydrate (283 mg, 0.77 mmol) were added dropwise to the solution. The saturated ethanol solution of sodium hydroxide was added dropwise to the mixture to adjust the pH to 7. After stirring 1 h, white precipitate was removed from the reaction mixture. The reaction solution was evaporated to yield a light-yellow powder. The obtained powder was recrystallized from acetonitrile to afford light-yellow crystals.

Yield: 510.5 mg, 45.0%.

Elemental analysis: calcd. for $C_{60}H_{76}EuF_{20}NO_8$, C 48.99, H 5.21, N 0.95; found, C 48.46, H 5.08, N 1.13%

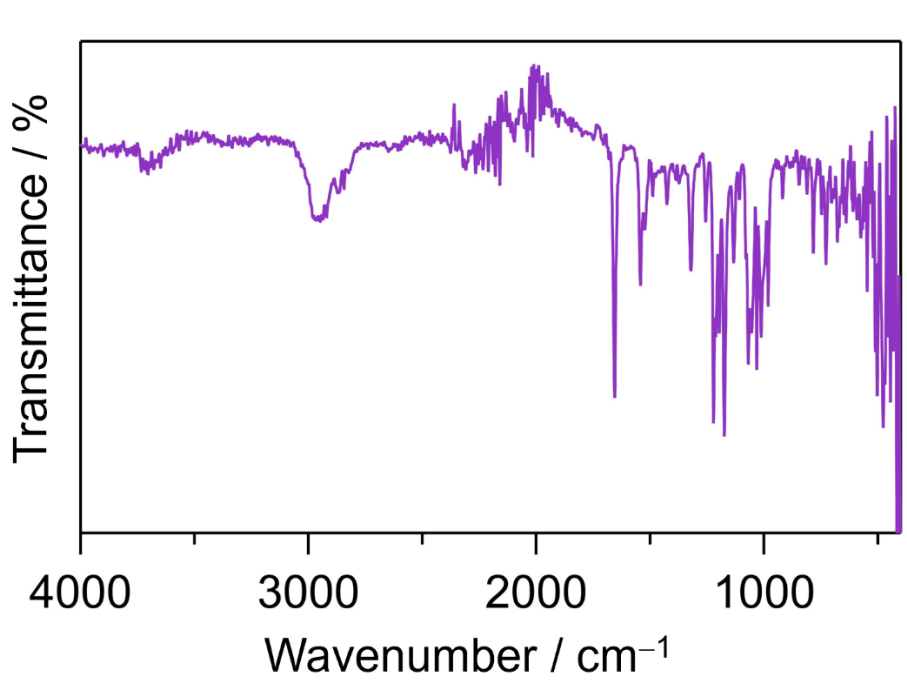

Figure S3. IR spectrum of TEA[Eu(+pfc)$_4$].

1.6 Preparation of mixed film composed of TEA[Eu(−tfc)$_4$] and TEA[Eu(+pfc)$_4$]

Mixed solutions (2 mL) containing TEA[Eu(−tfc)] and TEA[Eu(+pfc)] were prepared at three different molar ratios: (1) 1.33 mM : 0.67 mM, (2) 1.00 mM : 1.00 mM, and (3) 0.67 mM : 1.33 mM. These solutions were then analyzed by ESI-MS. The spectra revealed the formation of [Eu(−tfc)$_n$(+pfc)$_{4-n}$] (n = 0–4) (Figures S4–S6).

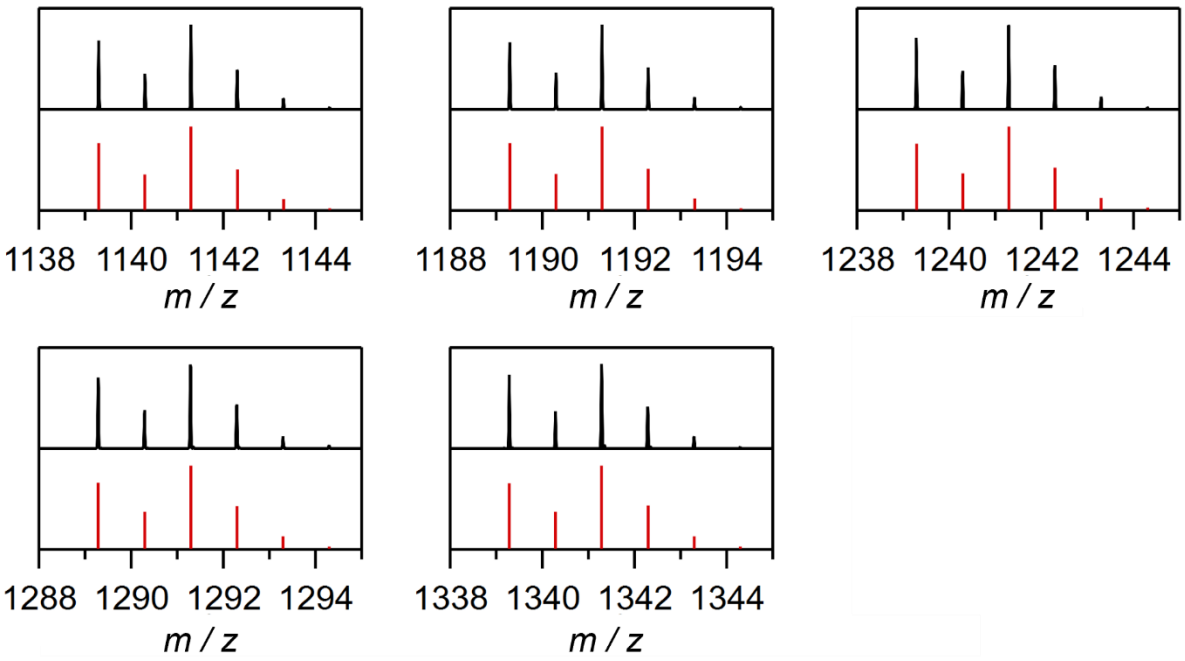

Figure S4. ESI-MS spectra for mixed solution (TEA[Eu(−tfc)$_4$]: 1.33 mM and TEA[Eu(+pfc)$_4$]: 0.67 mM). Black lines and red bars show experimental and simulated spectra, respectively. *m*/z calcd. for $C_{48}H_{56}EuF_{12}O_8$ ([Eu(−tfc)$_4$]$^-$), 1141.30; found, 1141.30. *m*/z calcd. for $C_{49}H_{56}EuF_{14}O_8$ ([Eu(−tfc)$_3$(+pfc)$_1$]$^-$), 1191.30; found, 1191.30. *m*/z calcd. for $C_{50}H_{56}EuF_{16}O_8$ ([Eu(−tfc)$_2$(+pfc)$_2$]$^-$), 1241.30; found, 1241.29. *m*/z calcd. for $C_{51}H_{56}EuF_{18}O_8$ ([Eu(−tfc)$_1$(+pfc)$_3$]$^-$), 1291.29; found, 1291.29. *m*/z calcd. for $C_{52}H_{56}EuF_{20}O_8$ ([Eu(+pfc)$_4$]$^-$), 1341.29; found, 1341.29.

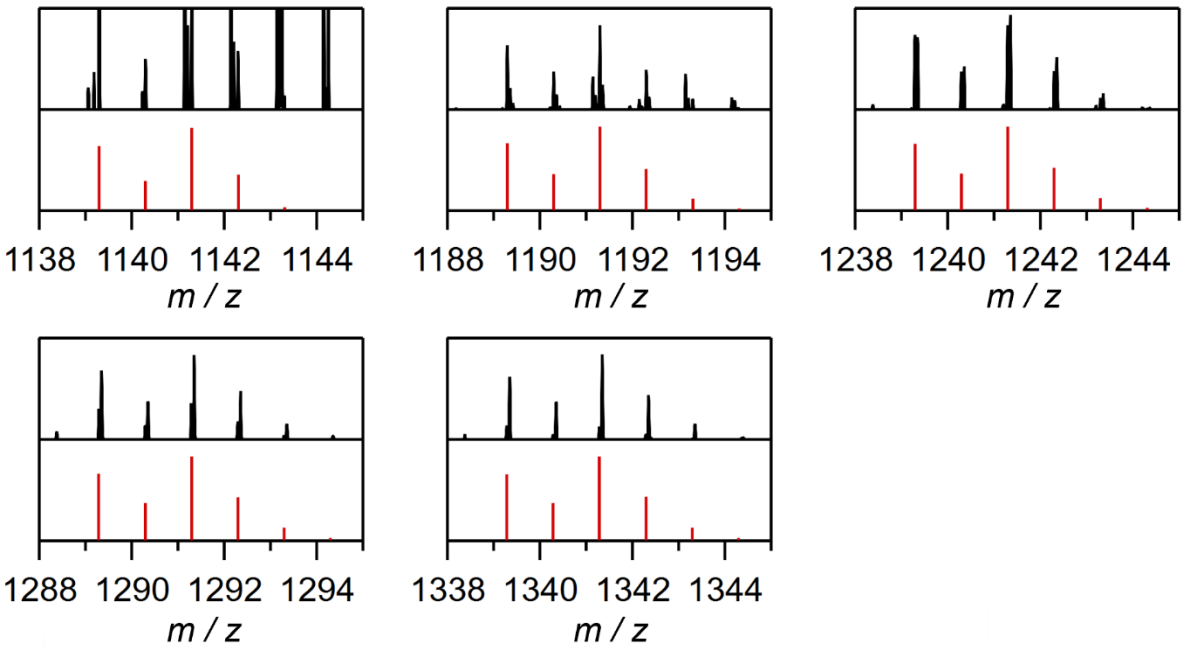

Figure S5. ESI-MS spectra for mixed solution (TEA[Eu(−tfc)$_4$]: 1.00 mM and TEA[Eu(+pfc)$_4$]: 1.00 mM). Black lines and red bars show experimental and simulated spectra, respectively. *m*/z calcd. for $C_{48}H_{56}EuF_{12}O_8$ ([Eu(−tfc)$_4$]$^-$), 1141.30; found, 1141.30. *m*/z calcd. for $C_{49}H_{56}EuF_{14}O_8$ ([Eu(−tfc)$_3$(+pfc)$_1$]$^-$), 1191.30; found, 1191.30. *m*/z calcd. for $C_{50}H_{56}EuF_{16}O_8$ ([Eu(−tfc)$_2$(+pfc)$_2$]$^-$), 1241.30; found, 1241.29. *m*/z calcd. for $C_{51}H_{56}EuF_{18}O_8$ ([Eu(−tfc)$_1$(+pfc)$_3$]$^-$), 1291.29; found, 1290.8. *m*/z calcd. for $C_{52}H_{56}EuF_{20}O_8$ ([Eu(+pfc)$_4$]$^-$), 1341.29; found, 1341.28.

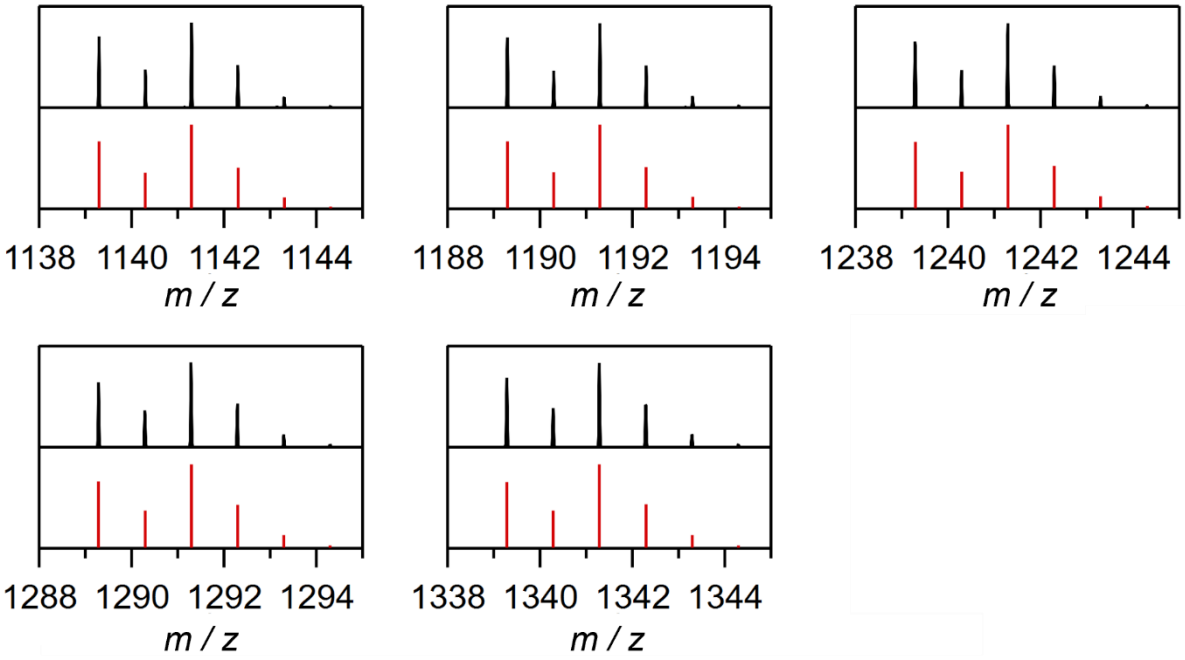

Figure S6. ESI-MS spectra for mixed solution (TEA[Eu(−tfc)$_4$]: 0.67 mM and TEA[Eu(+pfc)$_4$]: 1.33 mM). Black lines and red bars show experimental and simulated spectra, respectively. *m*/z calcd. for $C_{48}H_{56}EuF_{12}O_8$ ([Eu(−tfc)$_4$]$^-$), 1141.30; found, 1141.30. *m*/z calcd. for $C_{49}H_{56}EuF_{14}O_8$ ([Eu(−tfc)$_3$(+pfc)$_1$]$^-$), 1191.30; found, 1191.30 *m*/z calcd. for $C_{50}H_{56}EuF_{16}O_8$ ([Eu(−tfc)$_2$(+pfc)$_2$]$^-$), 1241.30; found, 1241.29. *m*/z calcd. for $C_{51}H_{56}EuF_{18}O_8$ ([Eu(−tfc)$_1$(+pfc)$_3$]$^-$), 1291.29; found, 1291.29. *m*/z calcd. for $C_{52}H_{56}EuF_{20}O_8$ ([Eu(+pfc)$_4$]$^-$), 1341.29; found, 1341.28.

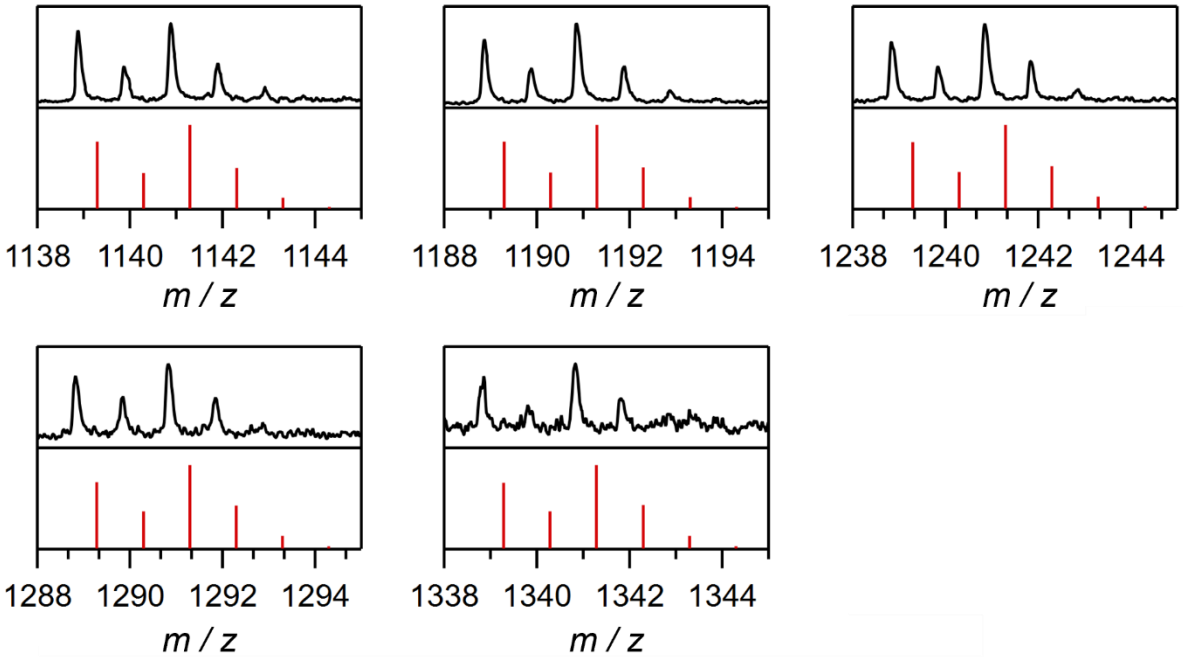

Figure S7. MALDI-TOF mass spectra of a mixed film prepared by casting solutions of TEA[Eu(−tfc)$_4$] and TEA[Eu(+pfc)$_4$] at a molar ratio of 2:1, using dithranol as matrix. Black lines and red bars show experimental and simulated spectra, respectively. *m*/z calcd. for $C_{48}H_{56}EuF_{12}O_8$ ([Eu(−tfc)$_4$]$^-$), 1141.30; found, 1140.9. *m*/z calcd. for $C_{49}H_{56}EuF_{14}O_8$ ([Eu(−tfc)$_3$(+pfc)$_1$]$^-$), 1191.30; found, 1190.9. *m*/z calcd. for $C_{50}H_{56}EuF_{16}O_8$ ([Eu(−tfc)$_2$(+pfc)$_2$]$^-$), 1241.30; found, 1240.8. *m*/z calcd. for $C_{51}H_{56}EuF_{18}O_8$ ([Eu(−tfc)$_1$(+pfc)$_3$]$^-$), 1291.29; found, 1290.8. *m*/z calcd. for $C_{52}H_{56}EuF_{20}O_8$ ([Eu(+pfc)$_4$]$^-$), 1341.29; found, 1340.8

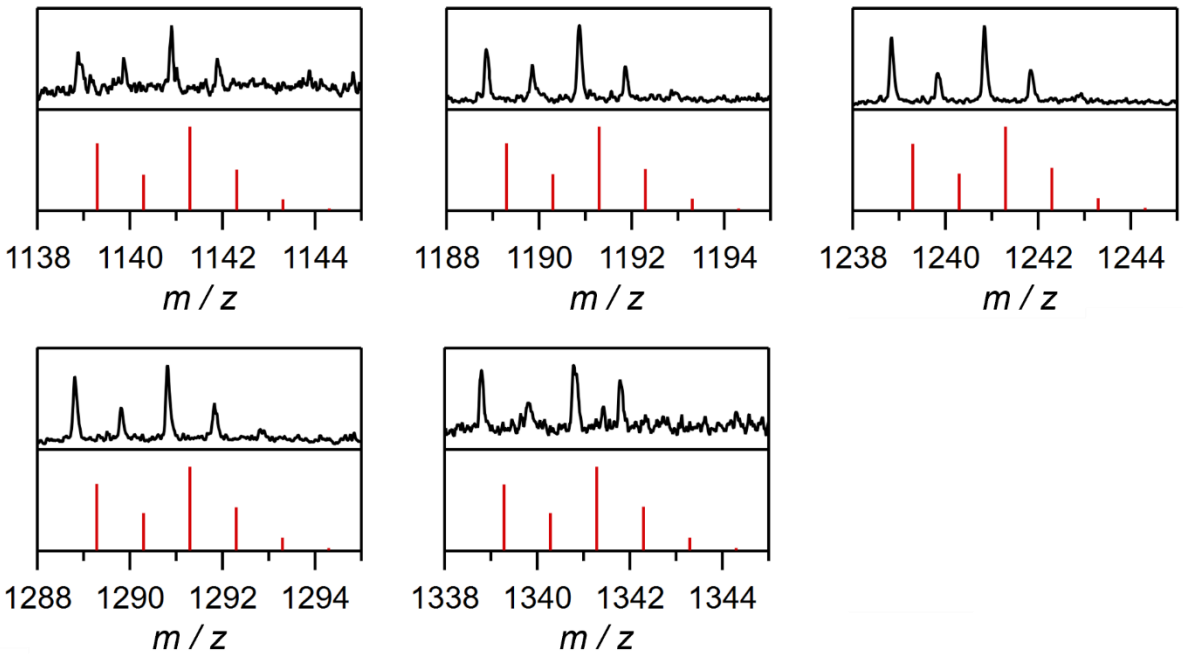

Figure S8. MALDI-TOF mass spectra of a mixed film prepared by casting solutions of TEA[Eu(−tfc)$_4$] and TEA[Eu(+pfc)$_4$] at a molar ratio of 1:1, using dithranol as matrix. Black lines and red bars show experimental and simulated spectra, respectively. *m*/z calcd. for $C_{48}H_{56}EuF_{12}O_8$ ([Eu(−tfc)$_4$]$^-$), 1141.30; found, 1140.9. *m*/z calcd. for $C_{49}H_{56}EuF_{14}O_8$ ([Eu(−tfc)$_3$(+pfc)$_1$]$^-$), 1191.30; found, 1190.9. *m*/z calcd. for $C_{50}H_{56}EuF_{16}O_8$ ([Eu(−tfc)$_2$(+pfc)$_2$]$^-$), 1241.30; found, 1240.8. *m*/z calcd. for $C_{51}H_{56}EuF_{18}O_8$ ([Eu(−tfc)$_1$(+pfc)$_3$]$^-$), 1291.29; found, 1290.8. *m*/z calcd. for $C_{52}H_{56}EuF_{20}O_8$ ([Eu(+pfc)$_4$]$^-$), 1341.29; found, 1340.8

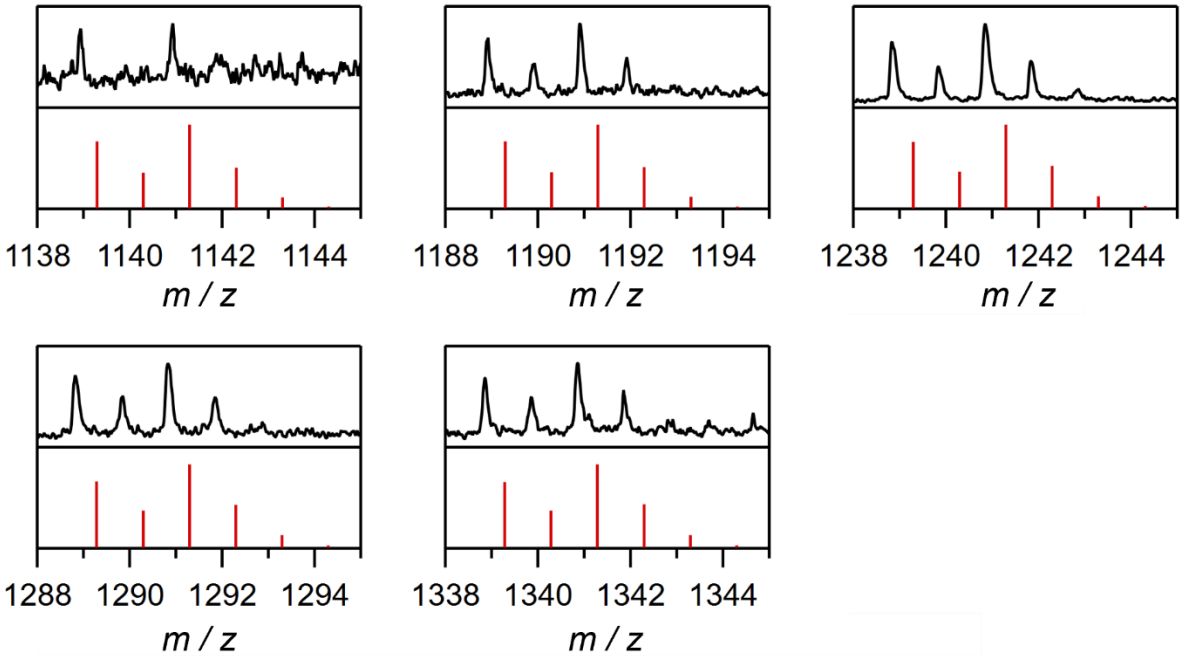

Figure S9. MALDI-TOF mass spectra of a mixed film prepared by casting solutions of TEA[Eu(−tfc)$_4$] and TEA[Eu(+pfc)$_4$] at a molar ratio of 1:2, using dithranol as matrix. Black lines and red bars show experimental and simulated spectra, respectively. *m*/z calcd. for $C_{48}H_{56}EuF_{12}O_8$ ([Eu(–tfc)$_4$]$^-$), 1141.30; found, 1140.9. *m*/z calcd. for $C_{49}H_{56}EuF_{14}O_8$ ([Eu(–tfc)$_3$(+pfc)$_1$]$^-$), 1191.30; found, 1190.9. *m*/z calcd. for $C_{50}H_{56}EuF_{16}O_8$ ([Eu(–tfc)$_2$(+pfc)$_2$]$^-$), 1241.30; found, 1240.8. *m*/z calcd. for $C_{51}H_{56}EuF_{18}O_8$ ([Eu(–tfc)$_1$(+pfc)$_3$]$^-$), 1291.29; found, 1290.9. *m*/z calcd. for $C_{52}H_{56}EuF_{20}O_8$ ([Eu(+pfc)$_4$]$^-$), 1341.29; found, 1340.9

1.7 Preparation of mixed film composed of TEA[Eu(–tfc)$_4$], TEA[Eu(+pfc)$_4$] and Coumarin102

Mixed films were prepared from $CHCl_3$ solutions containing TEA[Eu(–tfc)$_4$] (3.3 mM), TEA[Eu(+pfc)$_4$] (6.7 mM), and Coumarin 102. The molar of Coumarin 102 was varied from 0.6 mM to 2.4 mM. In each case, the resulting solution was spin-coated onto a substrate at 1,000 rpm for 60 s.

1.8 Transparency of mixed films

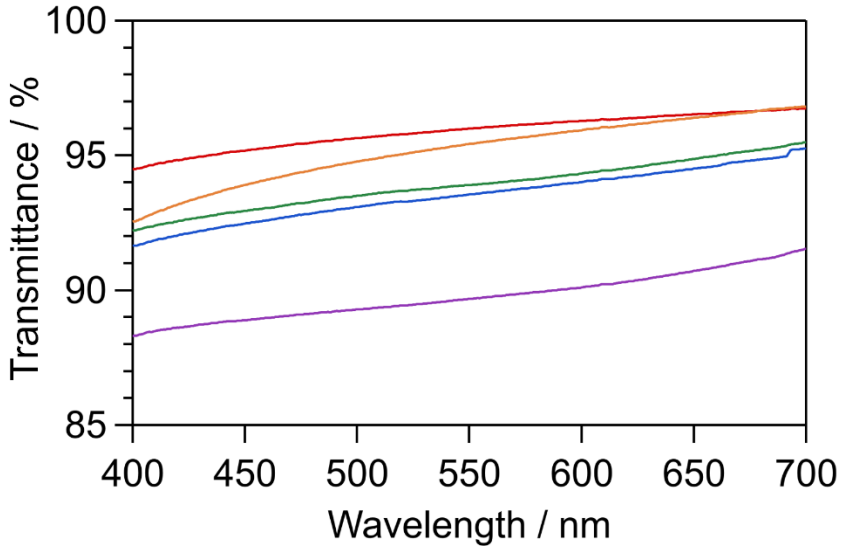

Figure S10. Transmission spectra of mixed films prepared by casting solutions of TEA[Eu(−tfc)$_4$] and TEA[Eu(+pfc)$_4$] at molar ratios of 2:1 (orange), 1:1 (green), and 1:2 (blue), along with the pure films of TEA[Eu(−tfc)$_4$] (red) and TEA[Eu(+pfc)$_4$] (purple).

1.9 Photophysical properties for Eu(III) films

Table S1. Emission lifetimes determined from emission decay curves (λ_{em} = 612 nm, Figure S19-23) and g_{CPL} values in $^5D_0 \rightarrow {}^7F_1$ transitions of Eu(III) films.

	Φ_{tot}[a] /%	$\Phi_{5D0\rightarrow7F1}$[a] /%	g_{CPL}[b]	τ_1 / μs	τ_2 / μs	τ_{avg} / μs
TEA[Eu(−tfc)$_4$]	3.83	0.36	1.38± 0.011	320 (0.64)	700 (0.36)	460
Mixed film (TEA[Eu(−tfc)$_4$] : TEA[Eu(+pfc)$_4$] = 2 : 1)	7.97	0.79	1.30± 0.029	390 (0.64)	870 (0.36)	640
Mixed film (TEA[Eu(−tfc)$_4$] : TEA[Eu(+pfc)$_4$] = 1 : 1)	11.9	0.98	1.52± 0.025	470 (0.21)	910 (0.79)	820
Mixed film (TEA[Eu(−tfc)$_4$] : TEA[Eu(+pfc)$_4$] = 1 : 2)	13.9	1.19	1.54± 0.006	580 (0.28)	926 (0.72)	830
TEA[Eu(+pfc)$_4$]	21.9	1.76	-	-	-	920[c]

[a] Φ_{tot} and $\Phi_{5D0\rightarrow7F1}$ denote the ligand-excited emission quantum yield for the $^5D_0 \rightarrow {}^7F_J$ (J = 0, 1, 2, 3, and 4) and $^5D_0 \rightarrow {}^7F_1$ transitions, respectively. λ_{ex}= 350 nm.

[b] The data represent the mean and standard deviation calculated from 12 measurements.

[c] The emission decay curve was fitted with a single exponential function (Figure S23).

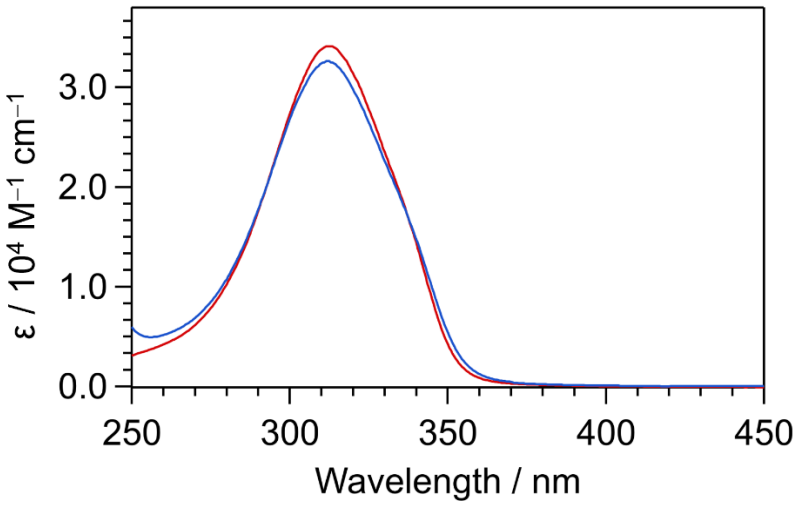

Figure S11. Absorption spectra of TEA[Eu(−tfc)$_4$] (red line) and a mixture of these complexes (TEA[Eu(−tfc)$_4$] : TEA[Eu(+pfc)$_4$] = 1 : 2) (blue line) in $CHCl_3$ solution (3×10^{-5} M).

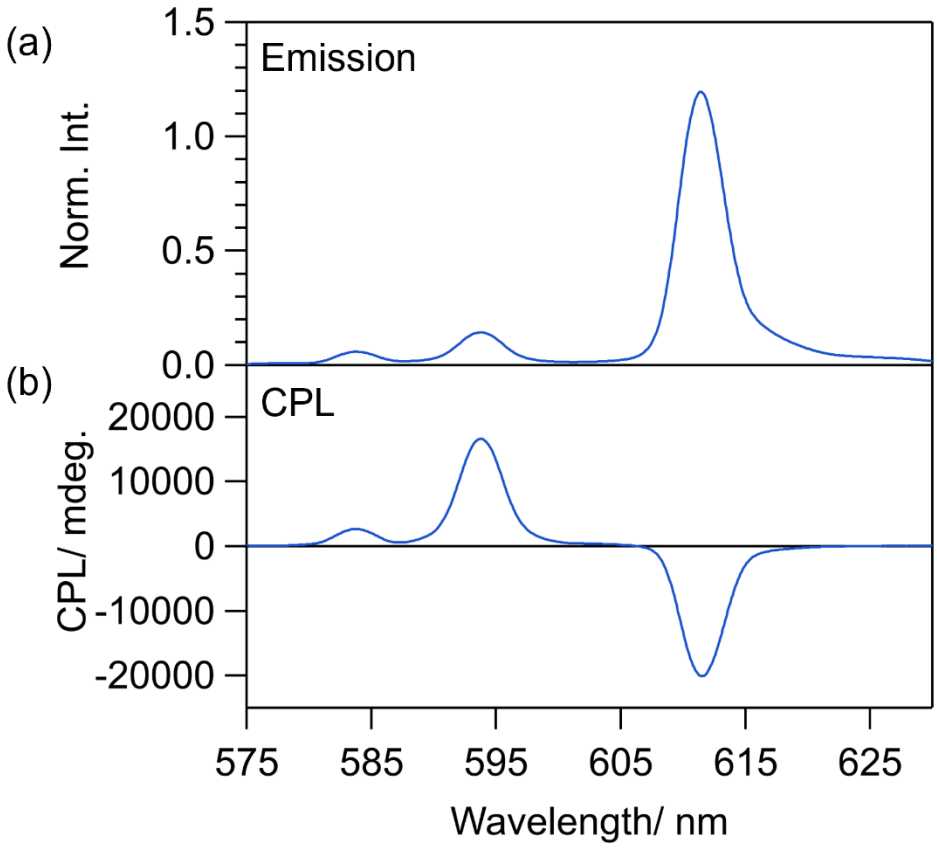

Figure S12. a) Emission and b) CPL spectra of a mixture of these complexes (TEA[Eu(−tfc)$_4$] : TEA[Eu(+pfc)$_4$] = 1 : 2) in $CHCl_3$ solution (2 mM, λ_{ex} = 350 nm) using CPL-300.

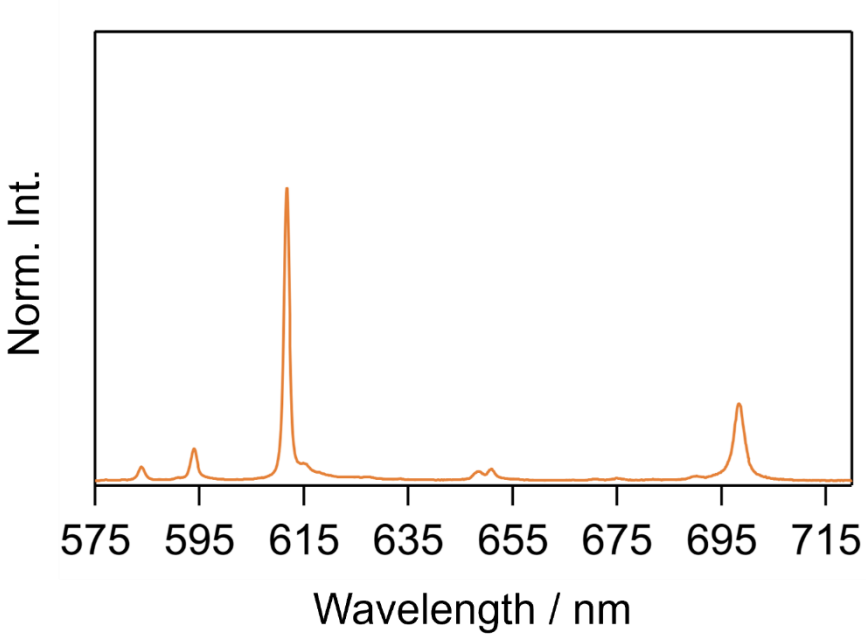

Figure S13. Emission spectrum of a mixed film prepared by casting $CHCl_3$ solution containing TEA[Eu(−tfc)$_4$] (1.33 mM) and TEA[Eu(+pfc)$_4$] (0.67 mM) (λ_{ex} = 350 nm).

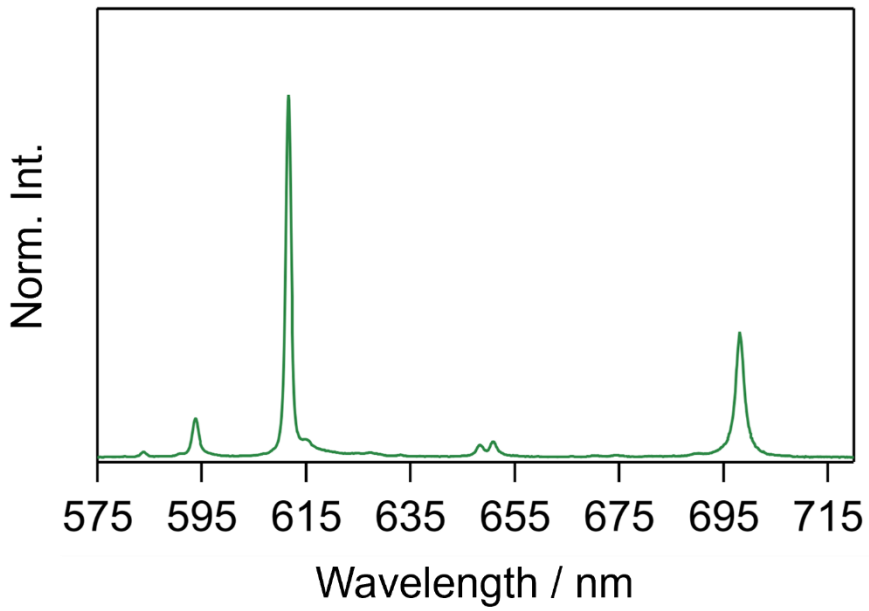

Figure S14. Emission spectrum of a mixed film prepared by casting $CHCl_3$ solution containing TEA[Eu(−tfc)$_4$] (1.0 mM) and TEA[Eu(+pfc)$_4$] (1.0 mM) (λ_{ex} = 350 nm).

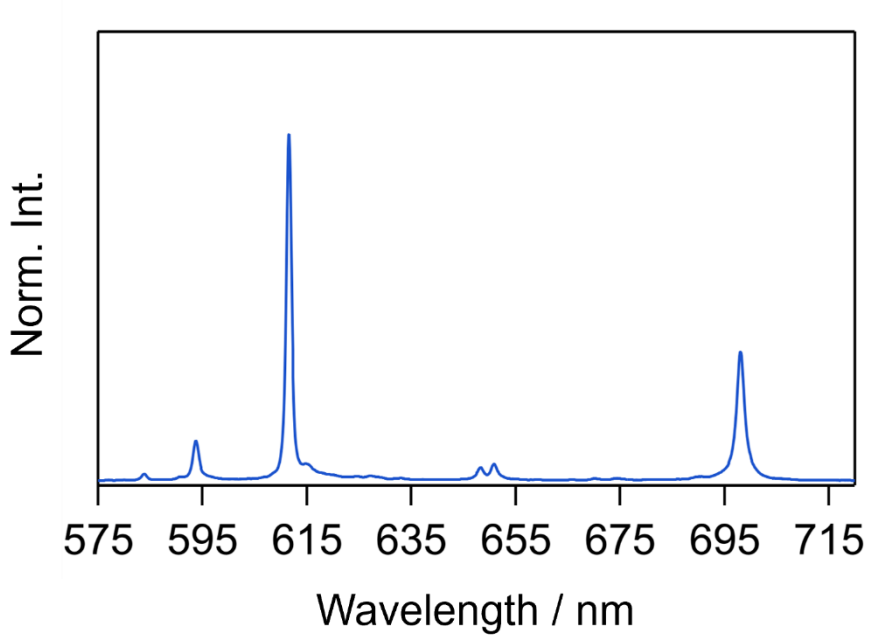

Figure S15. Emission spectrum of a mixed film prepared by casting $CHCl_3$ solution containing TEA[Eu(−tfc)$_4$] (0.67 mM) and TEA[Eu(+pfc)$_4$] (1.33 mM) (λ_{ex} = 350 nm).

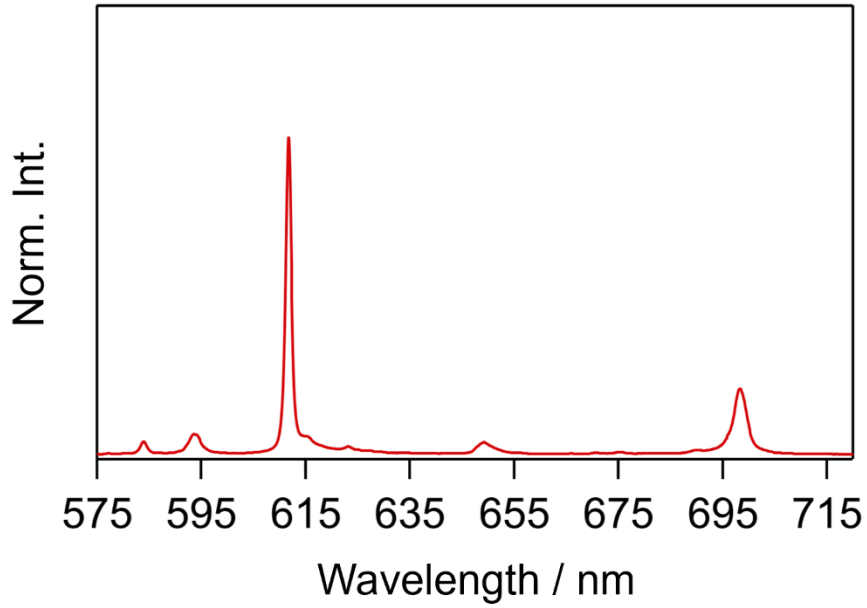

Figure S16. Emission spectrum of the pure film prepared by casting $CHCl_3$ solution containing TEA[Eu(−tfc)$_4$] (2.0 mM) (λ_{ex} = 350 nm).

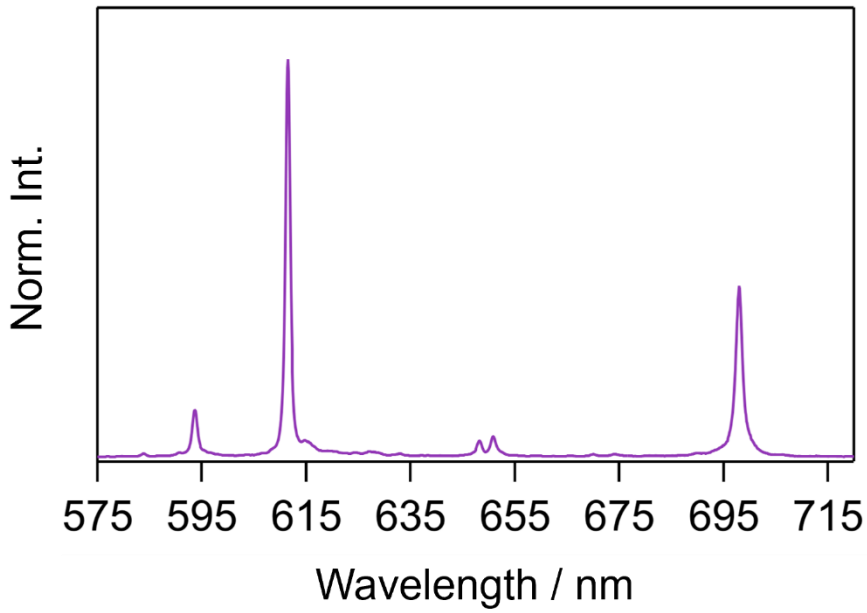

Figure S17. Emission spectrum of the pure film prepared by casting $CHCl_3$ solution containing TEA[Eu(+pfc)$_4$] (2.0 mM) (λ_{ex} = 350 nm).

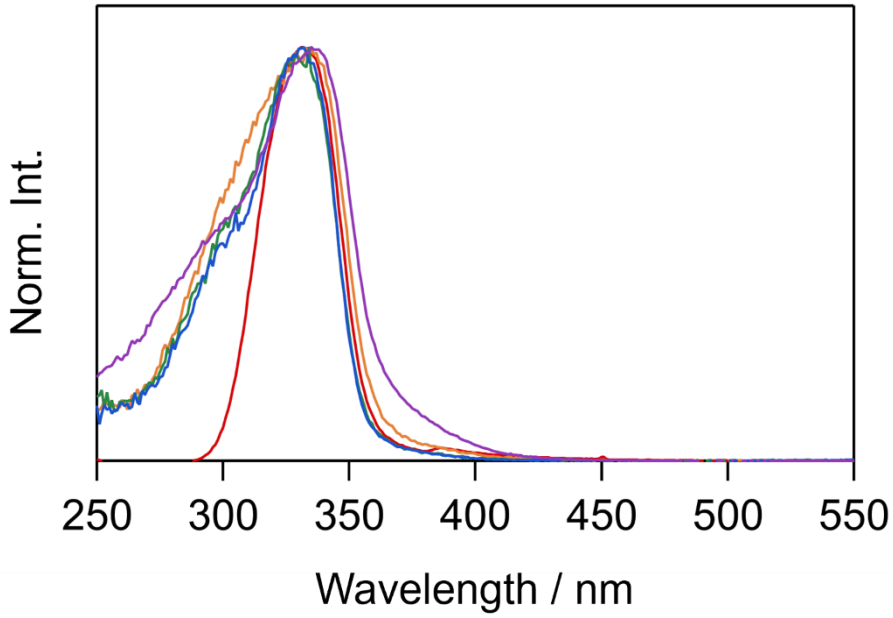

Figure S18. Excitation spectra of mixed films prepared by casting $CHCl_3$ solutions (total concentration: 2mM) containing TEA[Eu(−tfc)$_4$] and TEA[Eu(+pfc)$_4$] at molar ratios of 2:1 (orange), 1:1 (green), and 1:2 (blue), along with the pure films prepared by casting $CHCl_3$ solutions (concentration: 2mM) containing TEA[Eu(−tfc)$_4$] (red) or TEA[Eu(+pfc)$_4$] (purple), recorded at λ_{em} = 612 nm. Spectra are normalized to the intensity at 333 nm.

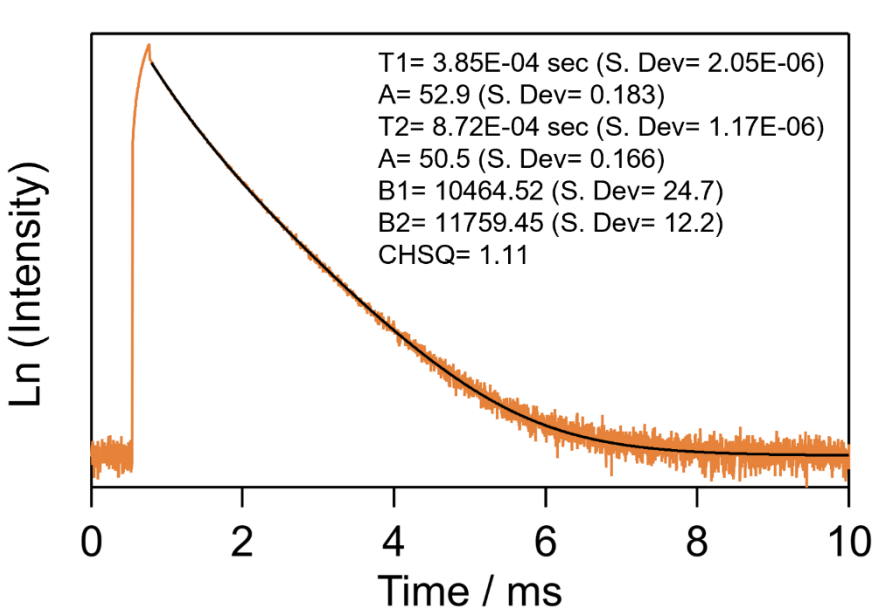

Figure S19. Emission decay curve of a mixed film prepared by casting $CHCl_3$ solutions containing TEA[Eu(−tfc)$_4$] (1.33 mM) and TEA[Eu(+pfc)$_4$] (0.67 mM) (orange line) and fitting curve (black line) (λ_{ex} = 356 nm, λ_{em} = 612 nm).

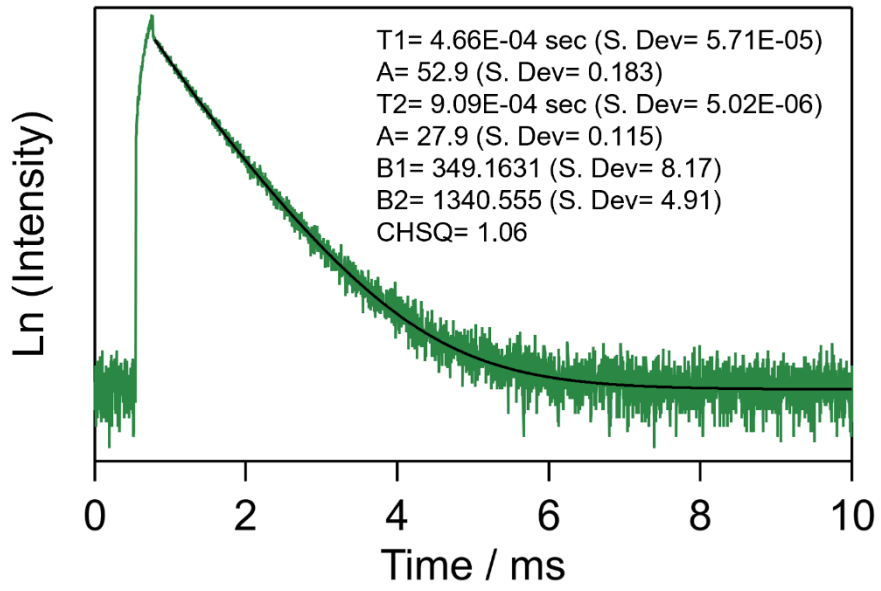

Figure S20. Emission decay curve of a mixed film prepared by casting $CHCl_3$ solutions containing TEA[Eu(−tfc)$_4$] (1.0 mM) and TEA[Eu(+pfc)$_4$] (1.0 mM) (green line) and fitting curve (black line) (λ_{ex} = 356 nm, λ_{em} = 612 nm).

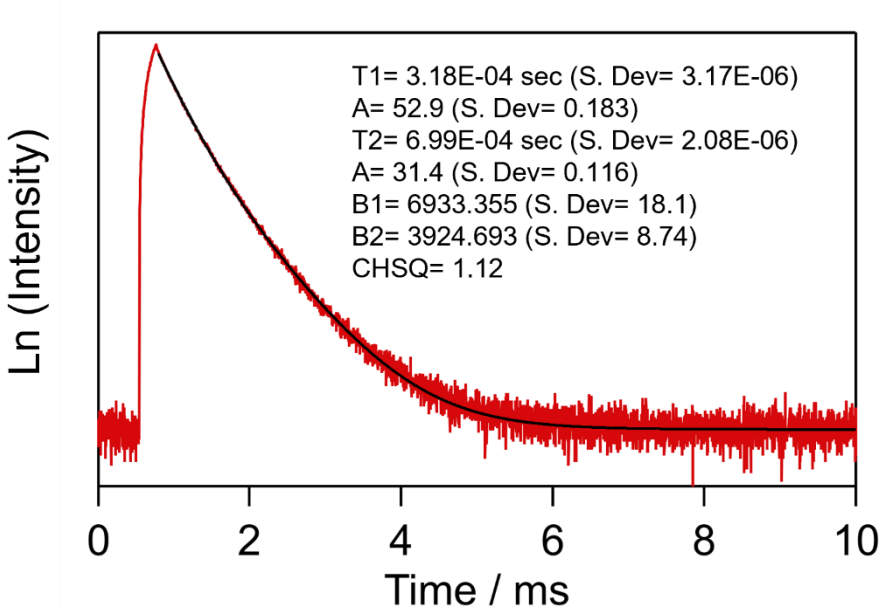

Figure S21. Emission decay curve of the pure film prepared by casting $CHCl_3$ solutions containing TEA[Eu(−tfc)$_4$] (2.0 mM) (red line) and fitting curve (black line) (λ_{ex} = 356 nm, λ_{em} = 612 nm).

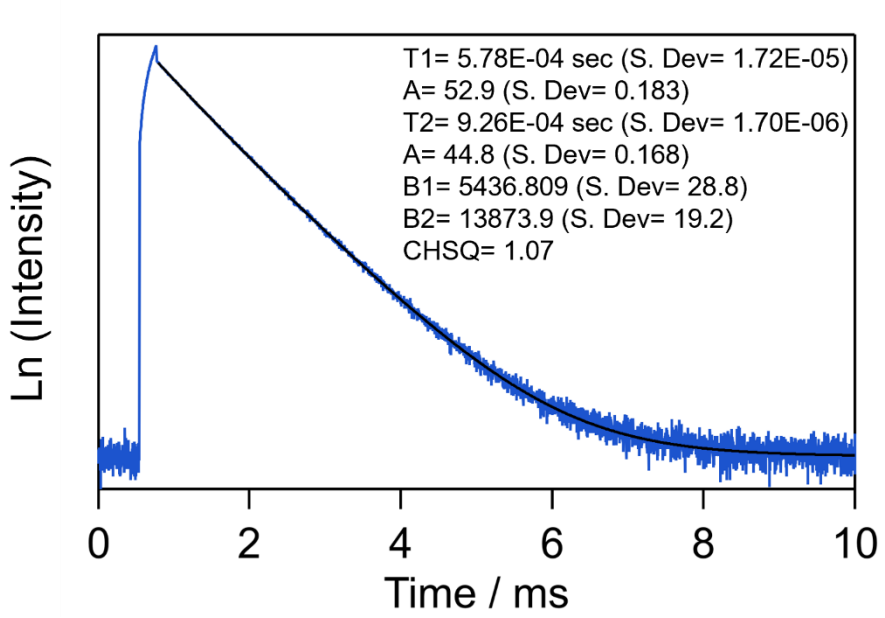

Figure S22. Emission decay curve of a mixed film prepared by casting $CHCl_3$ solutions containing TEA[Eu(−tfc)$_4$] (0.67 mM) and TEA[Eu(+pfc)$_4$] (1.33 mM) (blue line) and fitting curve (black line) (λ_{ex} = 356 nm, λ_{em} = 612 nm).

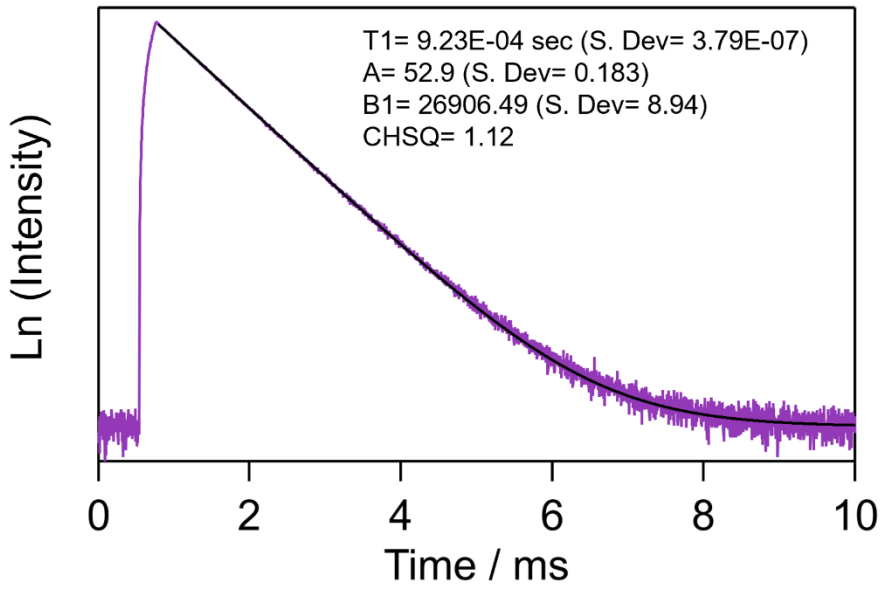

Figure S23. Emission decay curve of the pure film prepared by casting $CHCl_3$ solutions containing TEA[Eu(+pfc)$_4$] (2.0 mM) (purple line) and fitting curve (black line) (λ_{ex} = 356 nm, λ_{em} = 612 nm)

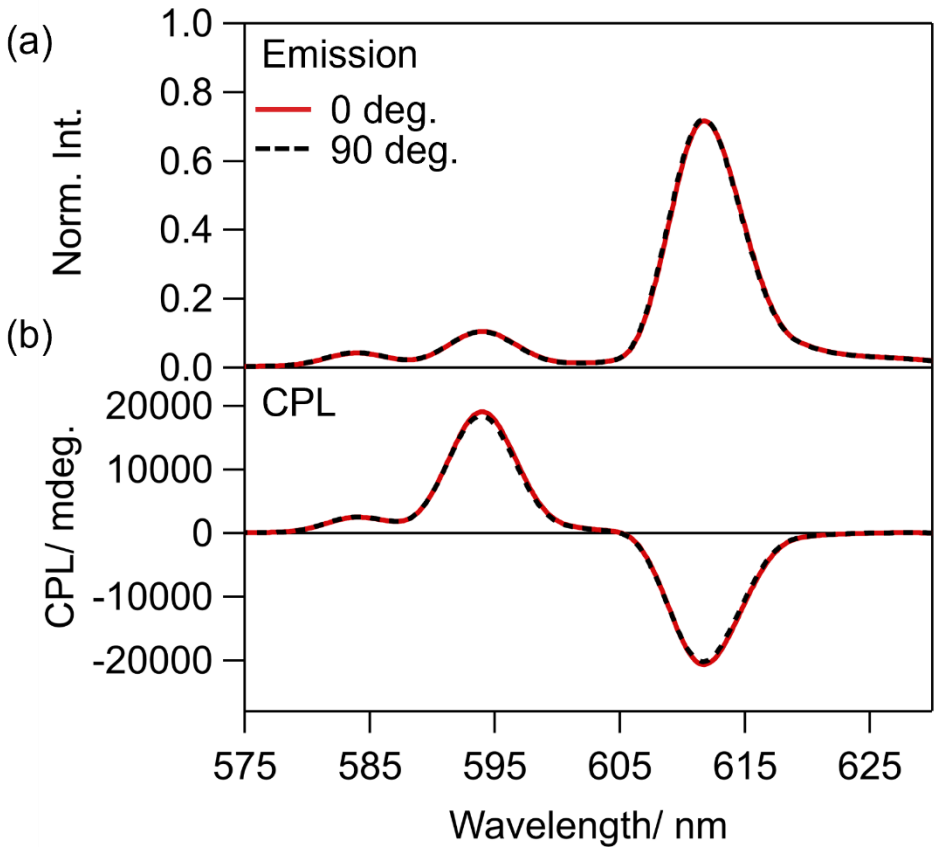

Figure S24. Rotation-dependent a) emission and b) CPL spectra of a mixed film prepared by casting $CHCl_3$ solutions containing TEA[Eu(−tfc)$_4$] (1.33 mM) and TEA[Eu(+pfc)$_4$] (0.67 mM). Emission spectra are normalized at emission area of $^5D_0 \rightarrow {}^7F_1$ transition.

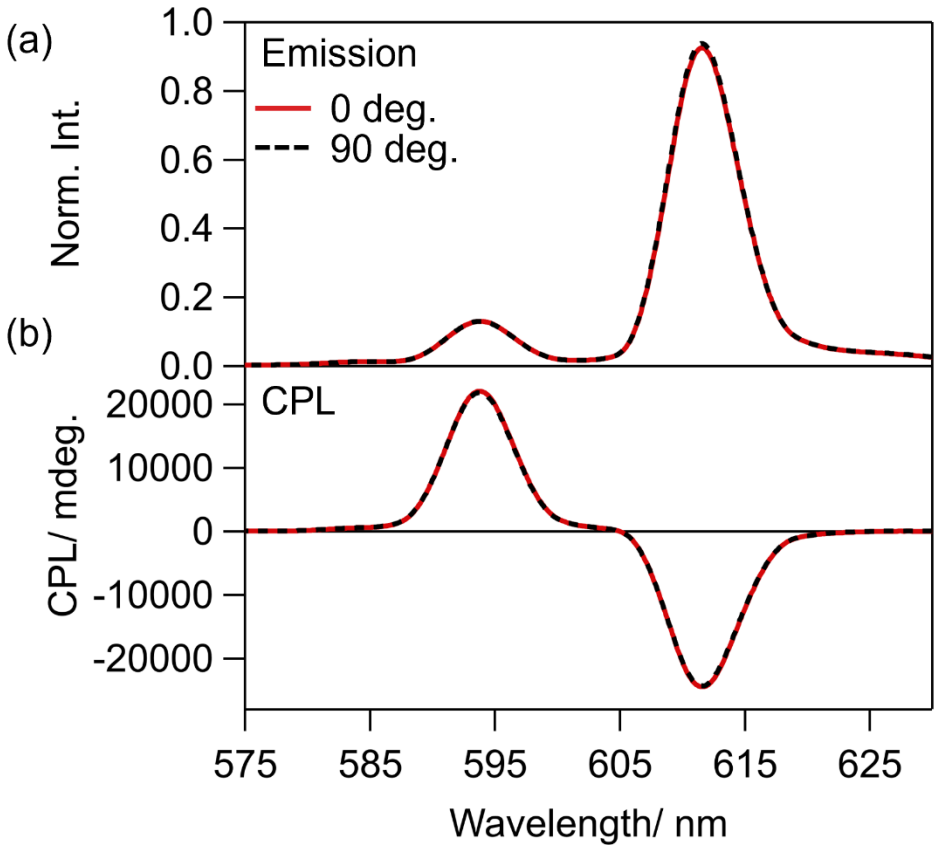

Figure S25. Rotation-dependent a) emission and b) CPL spectra of a mixed film prepared by casting $CHCl_3$ solutions containing TEA[Eu(−tfc)$_4$] (1.0 mM) and TEA[Eu(+pfc)$_4$] (1.0 mM). Emission spectra are normalized at emission area of $^5D_0 \rightarrow {}^7F_1$ transition.

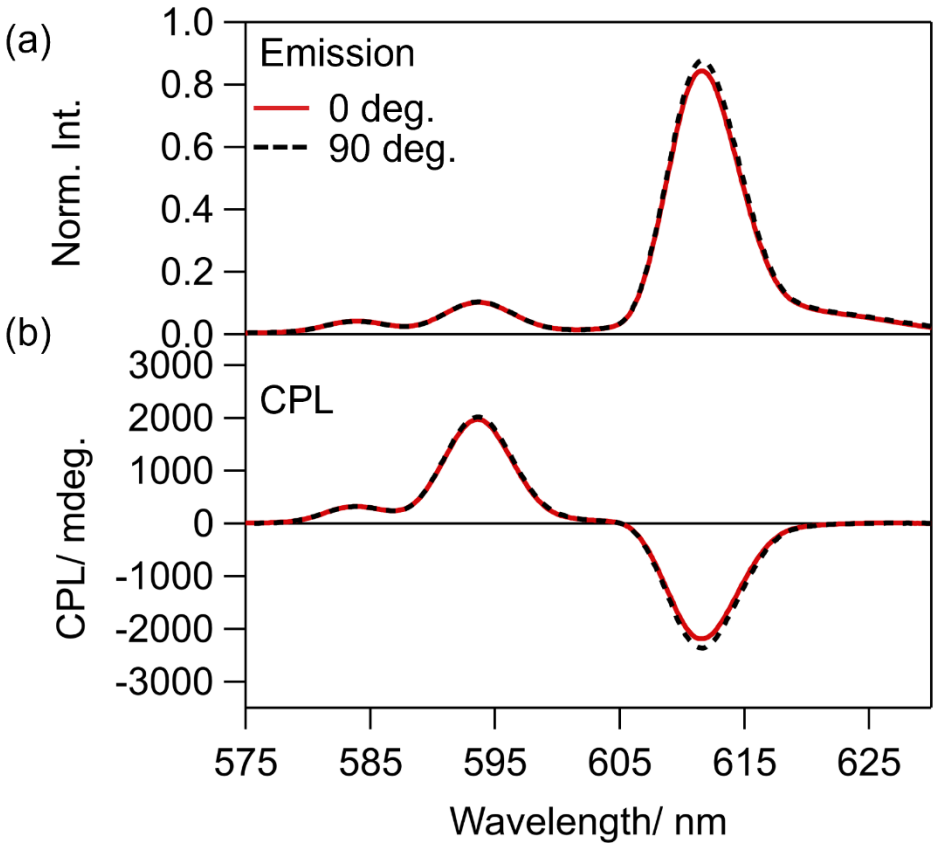

Figure S26. Rotation-dependent a) emission and b) CPL spectra of the pure film prepared by casting $CHCl_3$ solutions containing TEA[Eu(−tfc)$_4$] (2.0 mM) (λ_{ex} = 350 nm). Emission spectra are normalized at emission area of $^5D_0 \rightarrow {}^7F_1$ transition.

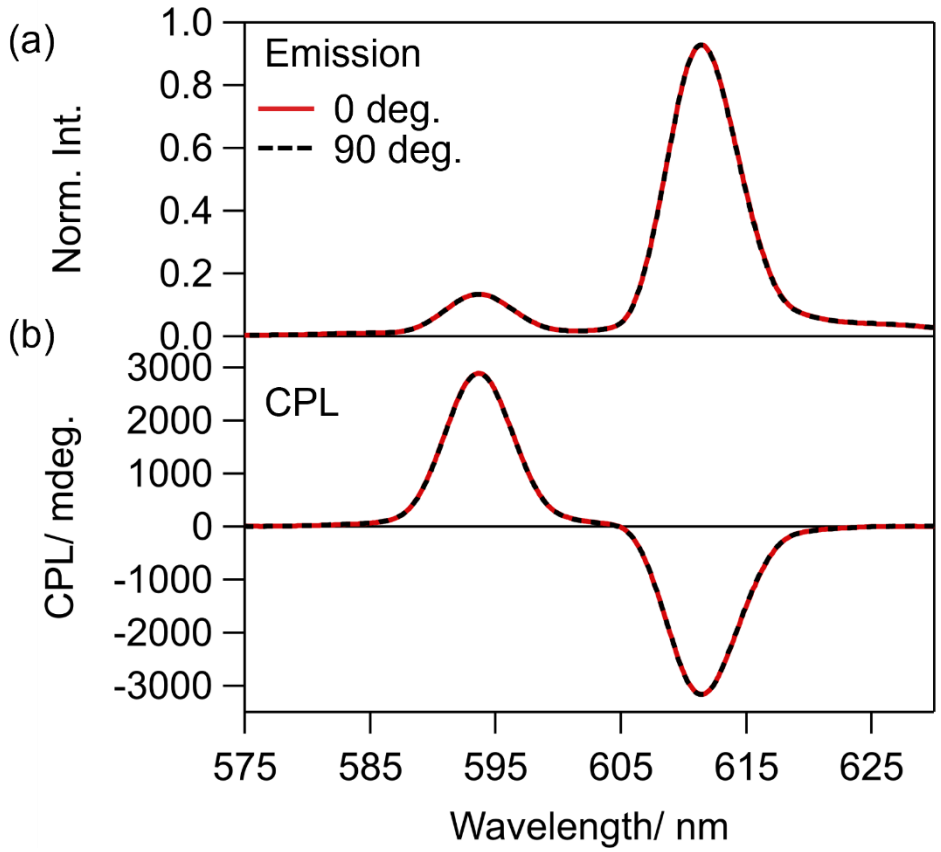

Figure S27. Rotation-dependent a) emission and b) CPL spectra of a mixed film prepared by casting $CHCl_3$ solutions containing TEA[Eu(−tfc)$_4$] (0.67 mM) and TEA[Eu(+pfc)$_4$] (1.33 mM). Emission spectra are normalized at emission area of $^5D_0 \rightarrow {}^7F_1$ transition.

1.10 CPL analyses for Eu(III) films

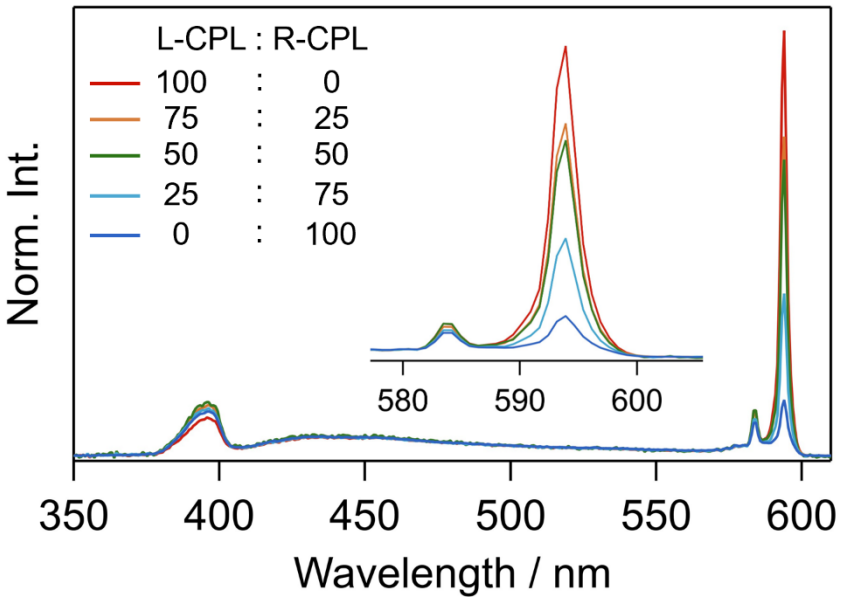

Figure S28. Emission spectra for an achiral Coumarin 102-doped **Eu-tfc/pfc-film** prepared on a glass substrate under UV light (λ_{ex} = 375 nm). The mixture has a molar ratio of 1:2:1.4 for TEA[Eu(−tfc)$_4$]:TEA[Eu(+pfc)$_4$] : Coumarin 102. The selective polarized emission was detected using the setup shown in Figure 1a with a Hamamatsu PMA-12 detector.

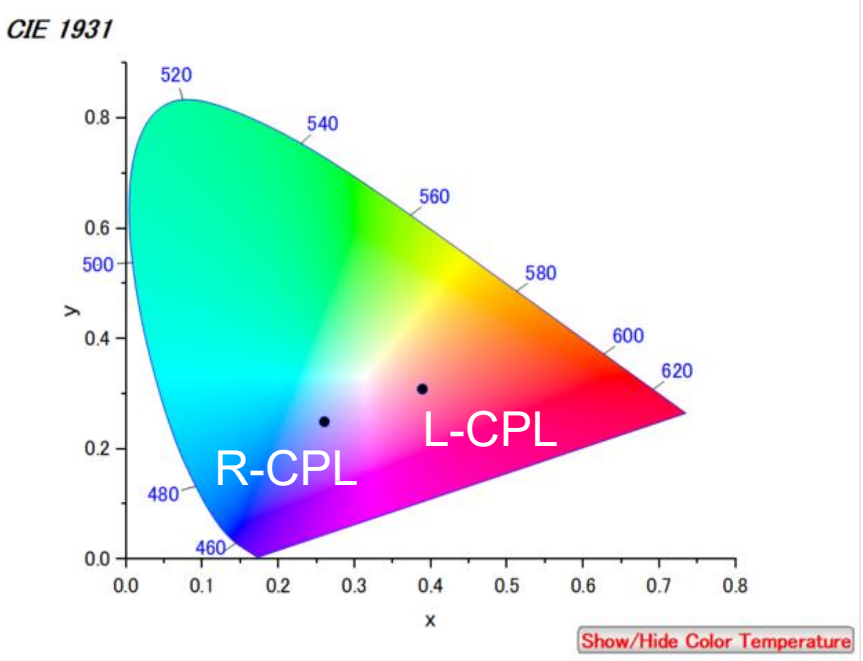

Figure S29. CIE chromaticity coordinates of L- and R-CPL, based on the spectra in Figure S29.

Table S2. CIE chromaticity coordinates, based on the spectra in Figure S30. The Euclidean distance between these two points in the color difference was calculated to be 0.142, which exceeds the threshold for human visual perception.

	x	y
L-CPL : R-CPL = 100 : 0	0.388762	0.309082
L-CPL : R-CPL = 75 : 25	0.364187	0.295870
L-CPL : R-CPL = 50 : 50	0.347442	0.290598
L-CPL : R-CPL = 25 : 75	0.311683	0.272972
L-CPL : R-CPL = 0 : 100	0.260059	0.249908

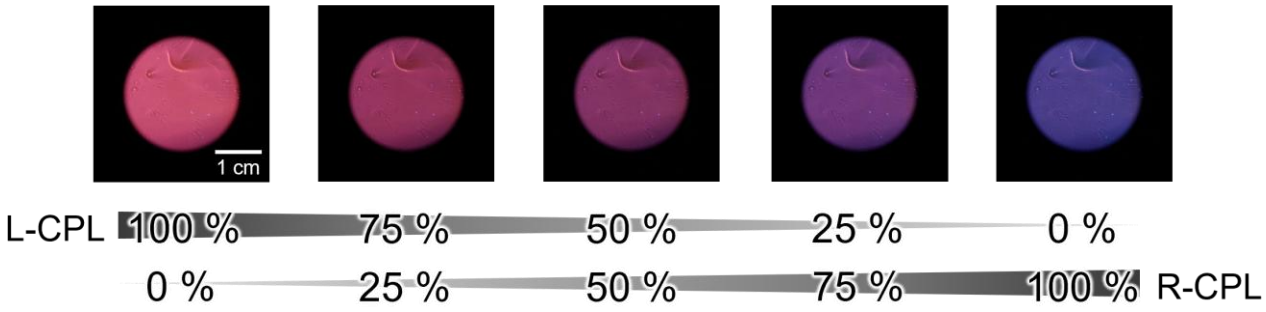

Figure S30. Photographs of an achiral Coumarin 102-doped **Eu-tfc/pfc-film** prepared on a glass substrate under UV light (λ_{ex} = 375 nm) with short-pass filter (< 400 nm), taken using the setup in Figure 1a (wavelength filter: short-pass, < 600 nm). The images from left to right correspond to L-CPL : R-CPL detection ratios of 100:0, 75:25, 50:50, 25:75, and 0:100, respectively. The mixture has a molar ratio of 1:2:0.34 for TEA[Eu(−tfc)$_4$]:TEA[Eu(+pfc)$_4$]:Coumarin 102.

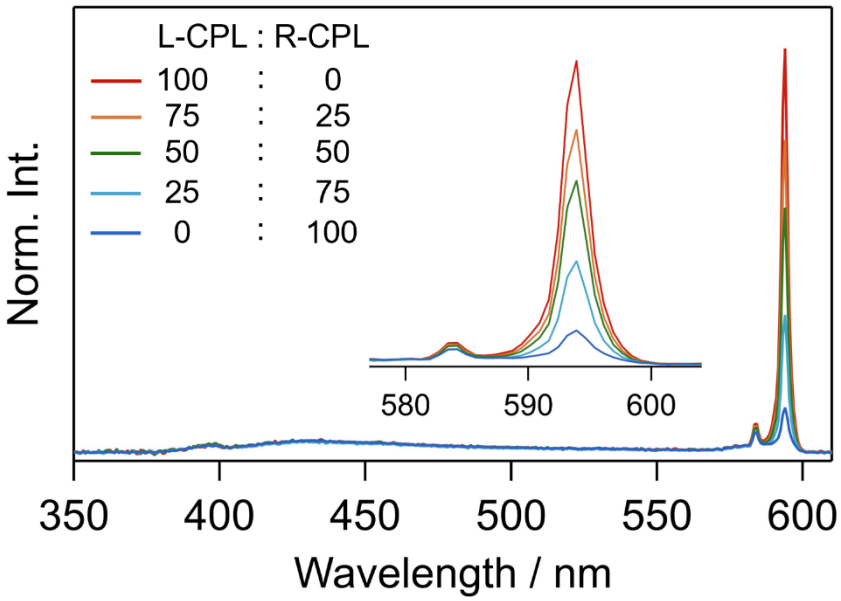

Figure S31. Emission spectra for an achiral Coumarin 102-doped **Eu-tfc/pfc-film** prepared on a glass substrate under UV light (λ_{ex} = 375 nm). The mixture has a molar ratio of 1:2:0.34 for TEA[Eu(−tfc)$_4$]:TEA[Eu(+pfc)$_4$]:Coumarin 102. The polarized emission was detected using the setup shown in Figure 1a with a Hamamatsu PMA-12 detector.

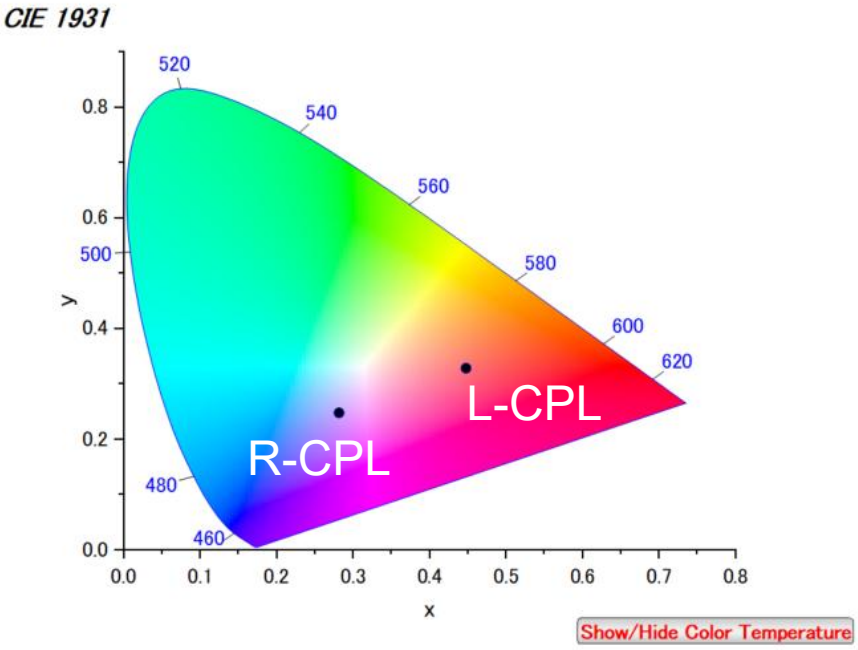

Figure S32. CIE chromaticity coordinates of L- and R-CPL, based on the spectra in Figure S31.

Table S3. CIE chromaticity coordinates, based on the spectra in Figure S32. The Euclidean distance between these two points in the color difference was calculated to be 0.184, which exceeds the threshold for human visual perception.

	x	y
L-CPL : R-CPL = 100 : 0	0.447121	0.328654
L-CPL : R-CPL = 75 : 25	0.421254	0.315053
L-CPL : R-CPL = 50 : 50	0.396560	0.305448
L-CPL : R-CPL = 25 : 75	0.356678	0.284452
L-CPL : R-CPL = 0 : 100	0.281237	0.237857

1.11 Energy transfer analyses for Eu(III) films

The time-resolved emission spectra of **Eu-tfc-film** and **Eu-tfc/pfc-film** are shown in Figure S33 and S34, respectively. The TRES spectra revealed two emission bands at approximately 530 and 540 nm, which were assigned to $^5D_1 \rightarrow {}^7F_0$ and $^5D_1 \rightarrow {}^7F_1$ transitions, respectively. The observation of $^5D_1$ emission bands revealed that photosensitization occurred via $^5D_1$. The emission decay curve revealed that the emission lifetime of $^5D_1$ in **Eu-tfc-film** (250 ns) is shorter than that in **Eu-tfc/pfc-film** (330 ns, Figure S35). This stabilization of the $^5D_1$ state suggests that the introduction of pfc ligands effectively suppresses non-radiative relaxation, which is caused by ligand-to-metal charge transfer (LMCT) quenching. This suppression of quenching pathways directly contributes to the enhancement of the ligand-excited emission quantum yield. These results provide experimental support for the enhanced B_{CPL} mechanism in the mixed film system.

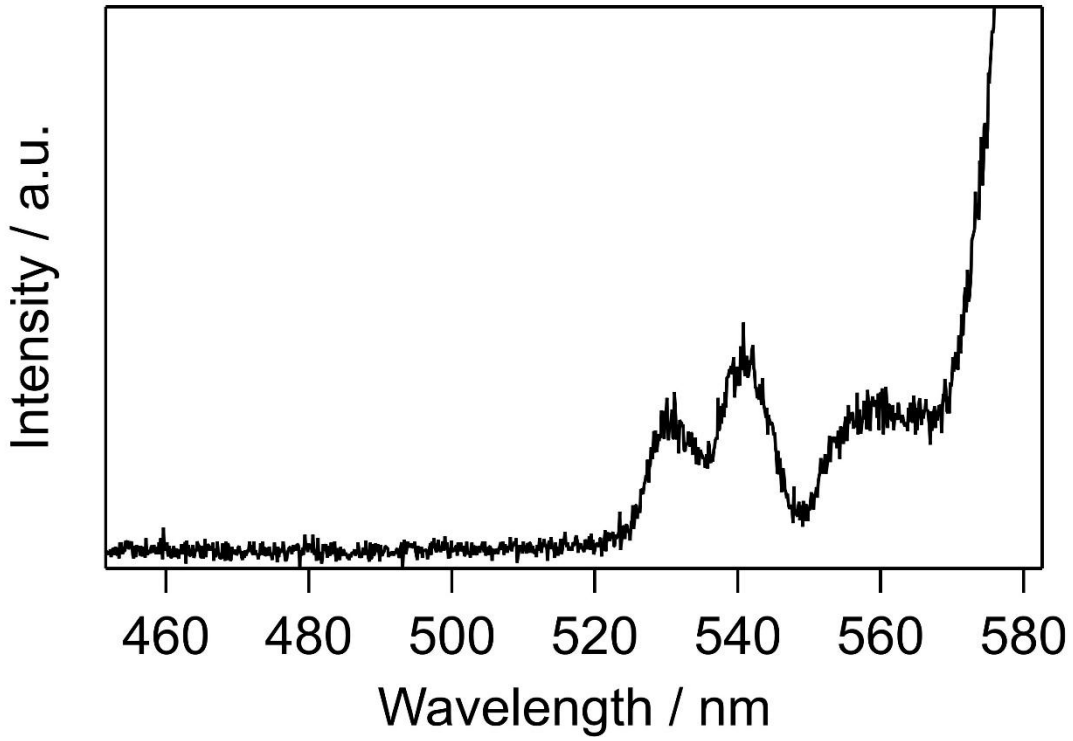

Figure S33. Time-resolved emission spectra of **Eu-tfc-film** (0–1.0 μs, λ_{ex} = 365 nm, in air).

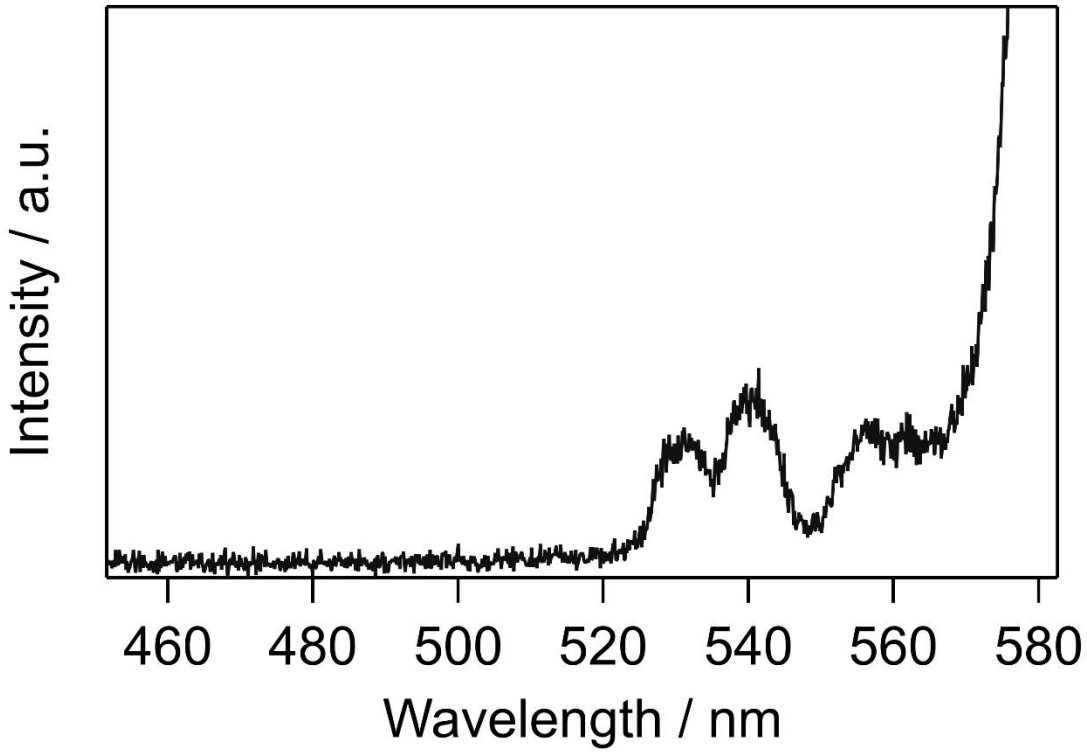

Figure S34. Time-resolved emission spectra of **Eu-tfc/pfc-film** (0–1.0 μs, λ_{ex} = 365 nm, in air).

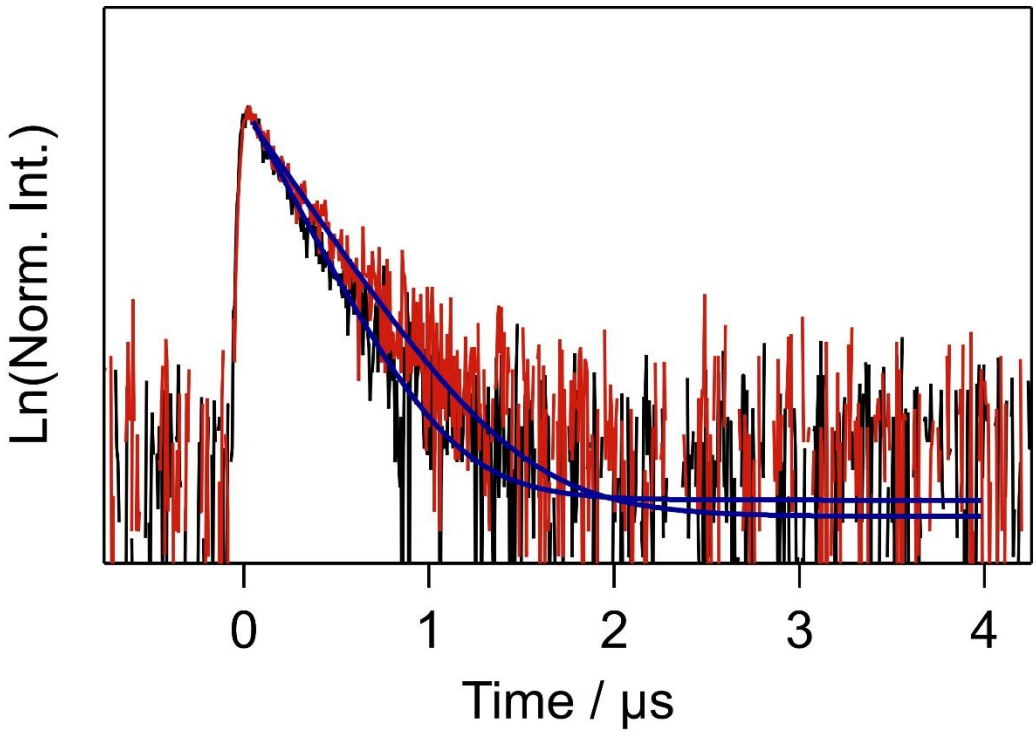

Figure S35. Emission decay curves (λ_{em} = 540 nm) of **Eu-tfc-film** (black line, λ_{ex} = 365 nm, in air) and **Eu-tfc/pfc-film** (red line, λ_{ex} = 365 nm, in air). Blue lines correspond to fitting curve.

References

20. Kitagawa, Y. et al. Chiral lanthanide lumino-glass for a circularly polarized light security device. *Commun. Chem.* **3**, 119 (2020).

24. Tsurui, M., Kitagawa, Y., Shoji, S., Fushimi, K. & Hasegawa, Y. Enhanced circularly polarized luminescence of chiral Eu(III) coordination polymers with structural strain. *Dalton Trans.* **52**, 796 (2023).